AJNR

Assessment of cerebral perfusion and arterial anatomy in hyperacute stroke with three-dimensional functional CT: early clinical results.

G J Hunter, L M Hamberg, J A Ponzo, F R Huang-Hellinger, P P Morris, J Rabinov, J Farkas, M H Lev, P W Schaefer, C S Ogilvy, L Schwamm, F S Buonanno, W J Koroshetz, G L Wolf and R G González

AJNR Am J Neuroradiol 1998, 19 (1) 29-37
http://www.ajnr.org/content/19/1/29

AJNR Am J Neuroradiol 19:29–37, January 1998

Assessment of Cerebral Perfusion and Arterial Anatomy in Hyperacute Stroke with Three-dimensional Functional CT: Early Clinical Results

George J. Hunter, Leena M. Hamberg, John A. Ponzo, Frank R. Huang-Hellinger, P. Pearse Morris, James Rabinov, Jeffrey Farkas, Michael H. Lev, Pamela W. Schaefer, Christopher S. Ogilvy, Lee Schwamm, Ferdinand S. Buonanno,Walter J. Koroshetz, Gerald L. Wolf, and R. Gilberto González

PURPOSE: **Our purpose was to determine the clinical feasibility of quantitative three-dimensional functional CT in patients with hyperacute stroke.**

METHODS: **Twenty-two patients who underwent clinically indicated CT angiography were studied: nine patients had no stroke, eight had mature stroke, and five had hyperacute stroke (less than 3 hours since ictus). Maps were obtained of perfused cerebral blood volume (PBV), and CT angiograms were generated by using standard techniques.**

RESULTS: **Normal PBV values (mean ± SEM) were 4.6 ± 0.15% in the gray matter, 1.75 ± 0.09% in the white matter, 2.91 ± 0.20% in the cerebellum, 3.18 ± 0.10% in the caudate, 2.84 ± 0.23% in the putamen, 2.92 ± 0.29% in the thalamus, and 1.66 ± 0.03% in the brain stem. For patients with mature stroke, ischemic changes were visible on noncontrast, contrast-enhanced, and PBV scans. In patients with hyperacute stroke, ischemic changes were either absent or subtle before contrast administration, but became apparent on contrast-enhanced scans. Quantitative PBV maps confirmed reduced regional perfusion. CT angiograms in the hyperacute group showed occlusion of vessels in locations appropriate to the PBV deficits seen.**

CONCLUSION: **Quantitative three-dimensional functional CT is feasible for patients with hyperacute stroke. It is performed by using helical CT techniques, and yields measures of cerebrovascular physiological function, which are useful in this patient population.**

The results of several randomized, prospective clinical trials have recently demonstrated the effectiveness of intravenous alteplase (recombinant tissue plasminogen activator) in the treatment of certain patients with acute stroke (1–3). The availability of a triage mechanism that could identify patients with cerebral ischemia and exclude those with strokelike symptoms but without cerebral ischemia is crucial (4). Currently, triage is performed with conventional computed tomography (CT), and patients with positive clinical findings but a negative CT study (ie, without hemorrhage) are considered for alteplase therapy. Parameters of cerebrovascular function that provide positive evidence of ischemia, such as cerebral blood flow (CBF) or perfused cerebral blood volume (PBV), are desirable.

Because helical CT is available in many hospitals, we sought a way to use this technology to obtain measurements of intracranial vascular pathophysiology at a high spatial and temporal resolution (5, 6). Initial work has been limited to detailed, first-pass studies of regional cerebrovascular parameters in a single section through the brain (5, 7). We describe the implementation of this three-dimensional functional CT technique in the evaluation of patients with hyperacute stroke and report its feasibility for use in an emergency department equipped with a helical CT scanner.

Methods

Quantitative maps of cerebral perfusion were obtained retrospectively from data sets that were collected in an unselected

Received March 17, 1997; accepted after revision June 30.

From the Departments of Radiology (G.J.H., L.M.H., J.A.P., F.R.H-H., P.P.M., J.R., J.F., M.H.L., P.W.S., G.L.W., R.G.G.), Neurology (L.S., F.S.B., W.J.K.), and Neurosurgery (C.S.O.), Massachusetts General Hospital and Harvard Medical School, Boston.

Address reprint requests to George J. Hunter, MD, Center for Imaging and Pharmaceutical Research and Division of Neuroradiology, Department of Radiology, Bldg 149, Charlestown Navy Yard, Boston, MA 02129.

patient population undergoing CT angiography. Data from 22 patients were available for postprocessing. Each study consisted of two axial CT data collections, obtained before and during the infusion of contrast material. From these data, absolute regional cerebral perfusion measures and large-vessel CT angiograms were obtained.

Patients and Study Protocol

All patients underwent clinically indicated CT angiography as requested by their physician of record. The data were divided into three groups: patients with no history of stroke; patients with known, established stroke; and patients with hyperacute stroke (interval between ictus and presentation less than 3 hours).

Data sets from the nine patients who had no history of stroke or cerebral ischemia were used to obtain normal values for PBV in different regions. Eight patients who had known, established stroke were studied for the presence of major-vessel occlusion. The data sets from these patients were used to confirm the feasibility of demonstrating areas and volumes of perfusion deficits in locations established by clinical examination and previous imaging studies. Five patients suffering hyperacute stroke were referred for evaluation of major-vessel occlusion at the time of presentation in the emergency department. Data from these studies were postprocessed independent of patient treatment in order to demonstrate the feasibility of obtaining further information concerning the extent and location of hypoperfused regions.

CT was performed on a helical scanner in the head-first, supine orientation. An 18-gauge antecubital cannula was inserted prior to the patient's entry into the scanner, and the patient's head was immobilized in the manufacturer-supplied head-holder by forehead and chin straps. A conventional, nonhelical, axial study was obtained first with contiguous 3-mm sections from the foramen magnum to the circle of Willis; thereafter, 5-mm sections were obtained to the vertex. Twenty-five seconds after the start of a power infusion of up to 100 mL of nonionic contrast material at 3 mL/s, a 1:1 pitched helical scan was obtained from the foramen magnum to the circle of Willis at 3 mm/s, and immediately thereafter from the circle of Willis to the vertex at 5 mm/s. The scanning parameters were 120 kilovolts (peak) and 240 mA, with a 512 $\times$ 512 image matrix and a 25-cm acquisition field of view. The delay of 25 seconds was chosen to ensure passage of contrast material into the venous circulation before the onset of scanning. In patients with atrial fibrillation, this delay should be prolonged to account for the reduced cardiac output and consequent delay in filling all the cerebral vasculature before imaging.

To minimize noise in the PBV maps, images were also reconstructed at 1-mm intervals with a 256 $\times$ 256 matrix using a soft filtered reconstruction technique supplied by the manufacturer. For subsequent CT angiographic production, data from the helical acquisitions were reconstructed at 1-mm intervals onto a 512 $\times$ 512 matrix. The CT angiograms were then produced by using multiprojection volume reconstruction or maximum intensity projection algorithms.

Data Analysis

On the basis of the contrast agent's dilution in the intravascular space, we determined the tissue blood volume fraction by measuring the concentration of the agent in both parenchyma and whole blood. The ratio of these concentrations represents the fractional PBV in tissue, which can be converted to PBV as a percentage of voxel volume (%PBV) as well as to absolute PBV (milliliters per 100 g of tissue) when tissue density is known. Correction was made for the change in small- versus large-vessel hematocrit. A literature value of 0.85 was used for this ratio (8). As some movement often occurred between the baseline and contrast data sets, a semiautomated registration technique was implemented to minimize the motion artifacts.

To calculate the concentration of the contrast agent in tissue, we subtracted the registered, noncontrast, baseline scans from the helical scans acquired during infusion of the contrast agent to determine the change in Hounsfield units (ΔHU) on a voxel-by-voxel basis. In the resultant subtraction images, the intensity of each voxel was linearly proportional to the concentration of contrast agent within the voxel. We were able to ascertain the concentration of contrast material in the blood by using the subtraction image, obviating invasive blood sampling during the study (9). The sagittal sinus, transverse sinuses, sigmoid sinuses, and jugular veins provided voxels entirely composed of blood, with no partial volume averaging of other tissues. A reference blood concentration from one of these locations was thus used for each section to permit normalization of the parenchymal concentration to an absolute value (%PBV). Production of the PBV maps was retrospective, and did not form part of the prospective patient management. Three of the authors produced all the maps. Evaluation of the noncontrast and contrast-enhanced images was prospective in every case, and took place in real time as the images appeared on the console. CT angiographic reconstruction was performed immediately after the acquisition was complete. These data were both used in triage by the authors.

For patients with no history of stroke, normal values for PBV in the gray and white matter, caudate, putamen, thalami, cerebellum, and brain stem were obtained by a region-of-interest (ROI) technique. For the patients with subacute or chronic stroke, pixelwise maps of PBV were produced and compared with the known regions of hypoperfusion present in individual patients. Large-vessel angiograms were also obtained and compared with the regions of parenchymal hypoperfusion. In the patients with hyperacute stroke, retrospective data analysis allowed PBV maps to be correlated with the CT angiographic results obtained at the time of presentation in the emergency department.

The ROI technique used throughout the study was based on anatomy. Irregular ROIs were drawn in the relevant areas, such as the sagittal sinus, caudate head, and so forth, and the pixel values from these regions were then extracted and used for subsequent computation.

Results

The nine patients with no history of stroke comprised six women and three men (mean age, 55 years; range, 36 to 82 years). Their hematocrit corrected values for %PBV were 4.6 $\pm$ 0.15% in the gray matter, 1.75 $\pm$ 0.09% in the white matter, 3.18 $\pm$ 0.10% in the caudate, 2.84 $\pm$ 0.23% in the putamen, 2.92 $\pm$ 0.29 in the thalami, 2.91 $\pm$ 0.20% in the cerebellum, and 1.66 $\pm$ 0.03% in the brain stem. These values are consistent with data obtained by single-photon emission CT and conventional CT in healthy volunteers (8, 10, 11). The values are also consistent with the single-section bolus tracking functional CT results reported in patients with Alzheimer disease (12).

CT angiograms and PBV maps were generated for the 13 patients who had stroke (six women, seven men; mean age, 69 years; range, 38 to 81 years). Perfusion deficits were identified in all patients. In seven of these patients, CT angiograms showed focal-vessel occlusion in a distribution consistent with the perfusion deficit present on the accompanying PBV map. In six patients, no focal-vessel lesion was identified.

In five patients with a proximal focal-vessel cutoff,

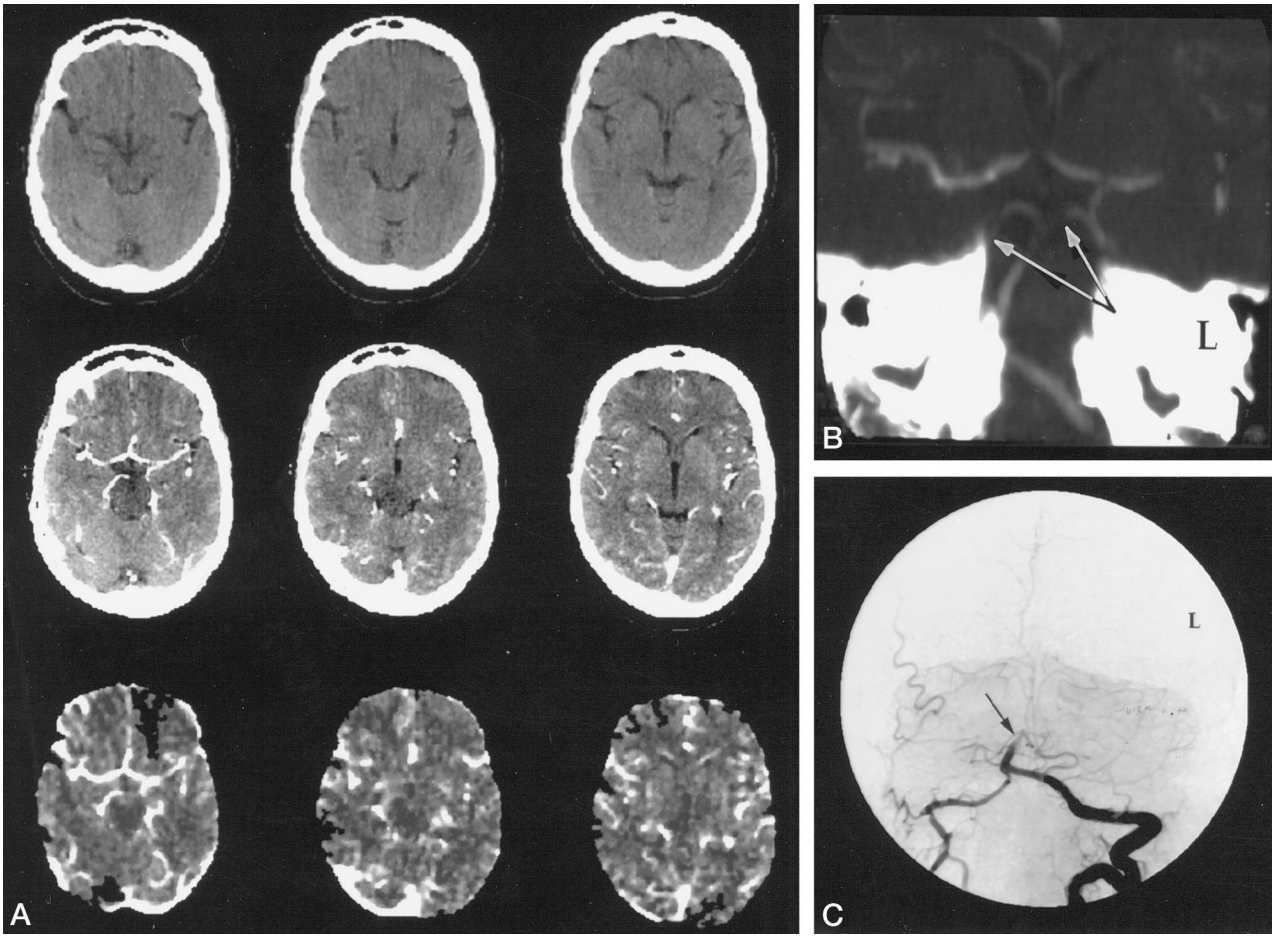

FIG 1. Patient 18.

A, Axial noncontrast (*upper row*) and contrast-enhanced (*middle row*) CT scans, and subtraction PBV maps (*bottom row*). Note decreased attenuation in the midbrain on the contrast-enhanced scans and subtraction images, which is not readily appreciable on the noncontrast scans. PBV was 0.49 ± 0.18%.

B, Collapsed multiprojection volume reconstruction in an oblique coronal plane from a CT angiogram shows filling defects in the distal basilar and posterior cerebral arteries (*arrows*).

C, Basilar artery occlusion (*arrow*) is identified on a conventional angiogram (left vertebral artery injection). The full extent of the thrombus is appreciated only on the CT angiogram, as a result of simultaneous opacification of all patent cerebral vessels as well as collateral pathways.

collateral flow was visualized on the CT angiograms (Figs 1 and 2). On the associated PBV maps, each of these patients had a perfusion deficit smaller than that seen in the single patient who had a similar large-vessel cutoff but no evidence of collateralization (Fig 3).

In the eight patients with established, mature infarctions, the baseline, noncontrast scans showed one or more areas of low attenuation. The contrast-enhanced scans showed decreased enhancement in the areas of infarction, and the PBV maps showed decreased perfusion in the same areas. In two patients with a history of stroke older than 3 months, the perfusion deficit on the PBV maps was less than expected. This suggests that the low-attenuation areas on the baseline scan included gliosis or scarring with partial revascularization, which was seen on the PBV maps as decreased, but not absent, perfusion (Fig 4).

In four patients with hyperacute neurologic deficits (cases 18 through 21, see the Table), confirmation of CT angiographic abnormalities was established by angiography before further interventional therapy was undertaken. In case 22, the lesion in the left posterior temporal lobe was small with no major-vessel cutoff on the CT angiogram (Fig 5). The patient did not proceed to emergency angiography and interventional therapy, but did undergo urgent diffusion-weighted magnetic resonance (MR) imaging, which confirmed the site and extent of ischemia (Fig 5).

Discussion

The rate of success of aggressive therapy for stroke would benefit from a simple technique for rapid identification of reduced parenchymal perfusion and major-vessel compromise (13). If, for example, a major-vessel occlusion is recognized sufficiently early, a patient may be referred for thrombolysis before irreversible cell death has occurred, at least in some of the affected brain (14, 15). The ability to identify a vascular lesion and to document recanalization and reperfusion should also aid future development of

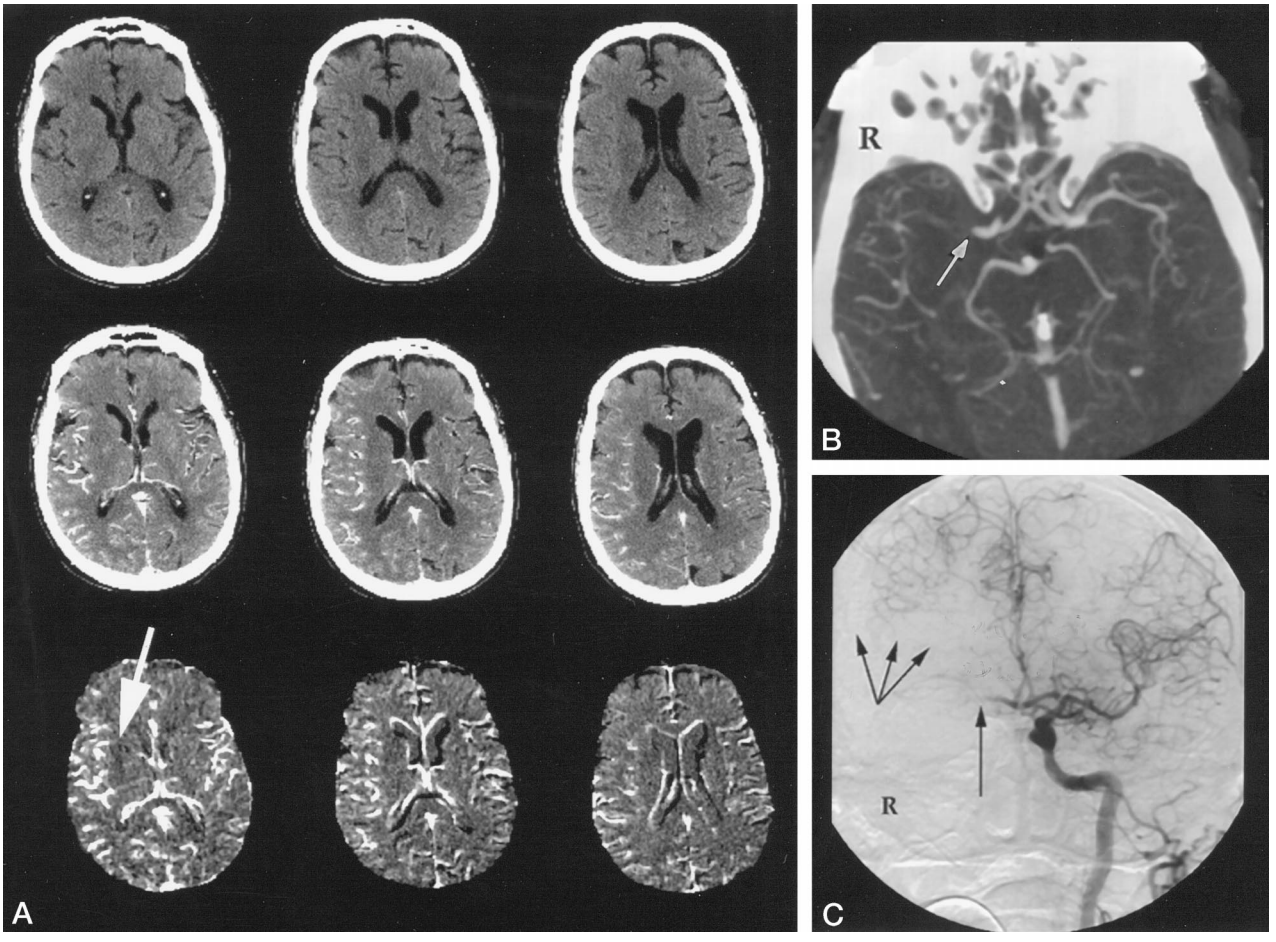

FIG 2. Patient 21.

A, Axial noncontrast (*upper row*) and contrast-enhanced (*middle row*) CT scans, and subtraction PBV maps (*bottom row*). Note decreased attenuation in the right internal capsule and corona radiata, seen most conspicuously on the subtraction images (*arrow*). PBV was 0.2 ± 0.06%.

B, Maximum intensity projection reconstruction from the CT angiogram shows an abrupt cutoff of the right MCA (*arrow*). Also seen is filling of distal right sylvian vessels resulting from collateral flow.

C, Conventional angiogram (left common carotid artery injection) shows cross-filling of the right A1 segment (*single arrow*), with collateral flow from branches of the anterior cerebral artery (ACA) to branches of the superior MCA (*triple arrows*).

effective thrombolytic agents and their means of administration. Most patients who have symptoms suggestive of cerebral ischemia or infarction undergo CT to exclude hemorrhage. In the current investigation, we used 3-D functional CT in a clinical setting to demonstrate its effectiveness in producing maps of PBV and CT angiograms of major vessels. A 3-D functional CT study, which is a conventional axial CT scan followed by an additional helical scan performed during power infusion of contrast material, can be completed in less than 20 minutes of patient table time.

Two major factors influence the quality of a 3-D functional CT study: the spatial resolution of image voxels and the amount of quantum noise present in an individual voxel. Quantum noise in a voxel is inversely related to the volume of the voxel, and is also influenced by the radiograph factors and reconstruction algorithm used to generate the CT scan. The signal that is being observed in 3-D functional CT is the ΔHU, generated by the arrival of iodine in a voxel following a power infusion of contrast material into a peripheral vein. Ultimately, it is the ΔHU-to-noise ratio that governs the ability to produce diagnostic PBV maps and CT angiograms.

In general, it is desirable to increase the spatial resolution of the images, particularly for the CT angiographic component of the 3-D functional CT study. Unfortunately, as the spatial resolution improves, the ΔHU-to-noise ratio deteriorates. One can compensate for this by increasing the radiograph factors used in the acquisition of the projection data, a strategy that is limited by the heat capacity of the X-ray tube. Alternatively, the observed ΔHU in a voxel may be increased by injecting a higher concentration of contrast agent more rapidly and in greater volume. This approach is limited by contrast dosage considerations.

For the CT angiographic component of a 3-D functional CT study, high spatial resolution can be retained without compromise because of the high contrast density in the voxels that comprise the blood vessels; ΔHU is at least 100, and often reaches values of 200 or greater. Under these conditions, the limiting

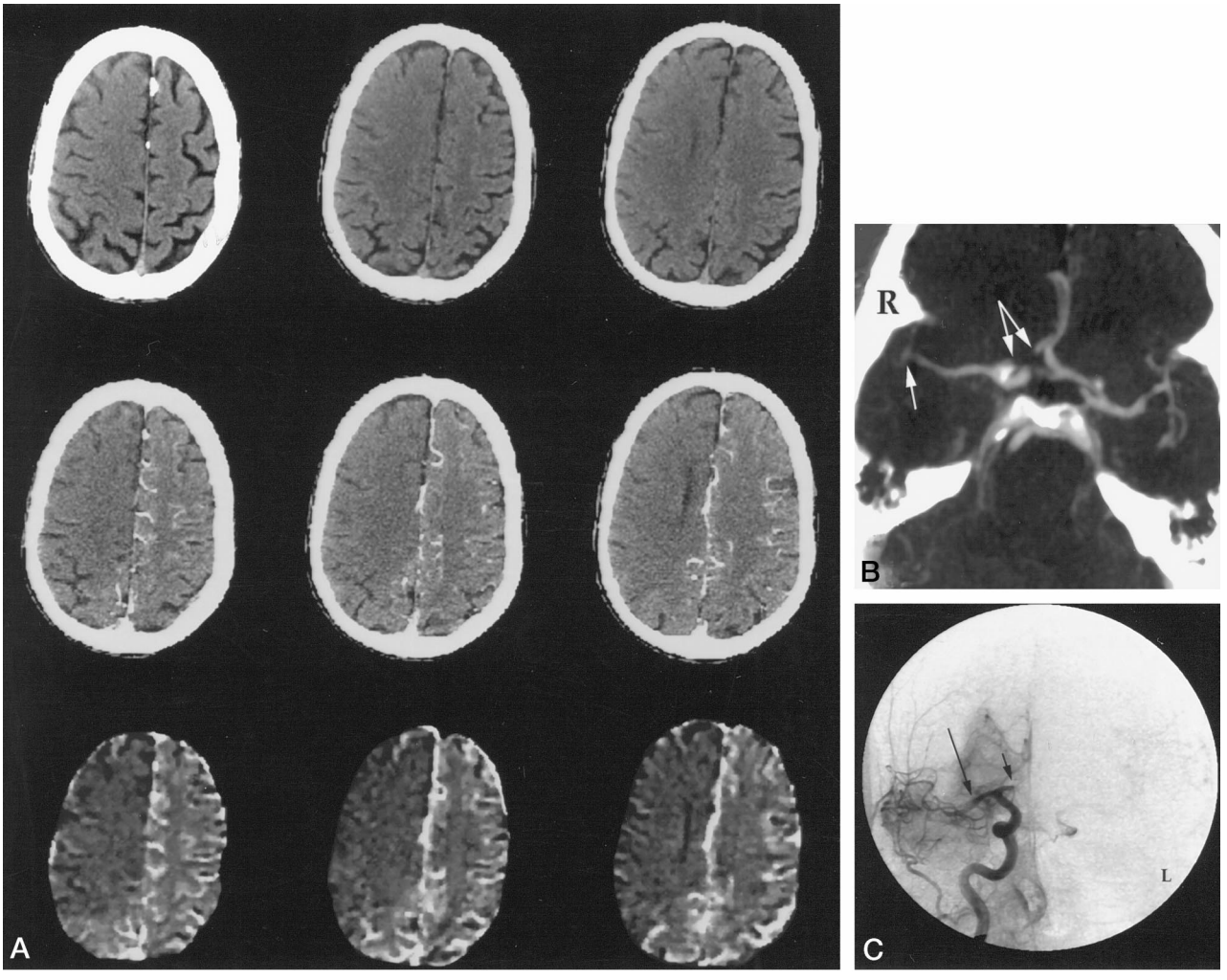

FIG 3. Patient 20.

A, Axial noncontrast (*upper row*) and contrast-enhanced (*middle row*) CT scans, and subtraction PBV maps (*bottom row*). Decreased attenuation involving the right anterior cerebral artery (ACA) and middle cerebral artery (MCA) territories of the brain are seen to best advantage on the contrast and subtraction images. PBV was 0.4 ± 0.04%. Also note increased conspicuity of right medial sulcal effacement on the contrast-enhanced images.

B, Collapsed multiprojection volume reconstruction from CT angiogram shows lack of contrast opacification in the right A1 segment (*double arrows*) and irregularity and poor filling in the distal right M1 segment and its branches (*single arrow*).

C, Conventional angiogram (right internal carotid artery injection) shows cutoff in the A1 segment of the right ACA and at the M1/M2 junction of the right MCA (*arrows*). No filling of the right ACA was seen.

factor is tube heat capacity. We obtained good-quality CT angiograms with factors of 120 kV(p), 240 mAs, and a section thickness of 3 mm through the circle of Willis, reconstructed on a 512 × 512 image matrix and reformatted at 1-mm intervals. These acquisition parameters alone, however, are insufficient to produce acceptable ΔHU-to-noise levels in the PBV maps. By reducing the in-plane spatial resolution to 1 mm, through the generation of images with a 256 × 256 matrix and the use of soft filter reconstruction, good-quality PBV maps were obtained as long as no movement occurred between the image sets being subtracted. Because some movement always occurs in patient studies, image registration is necessary in order to remove motion artifacts from the subtraction images.

In patients with normal cardiac output, we observed a ΔHU of between 5 and 10 in parenchymal voxels. To create a larger change in HU and improve signal-to-noise ratios, contrast concentration in each voxel should be maximized. If a patient must proceed immediately to intraarterial thrombolysis, with its attendant selective and superselective angiography, a legitimate concern arises regarding the total contrast load that may result from the 3-D functional CT procedure and subsequent digital subtraction angiography (DSA). Because we cannot identify such patients before contrast material is administered, we must assume that all patients will proceed to DSA. In recognition of this, our protocol calls for only 100 mL of contrast material at a concentration of 300 mg/mL of organic iodine. In the presence of normal creatinine levels, and as long as hydration is maintained, such a load should not cause any dose-related problems with renal function (16, 17).

During occlusive brain infarction or ischemia, local factors and altered biochemical pathways produce maximal dilatation of blood vessels (18, 19). This

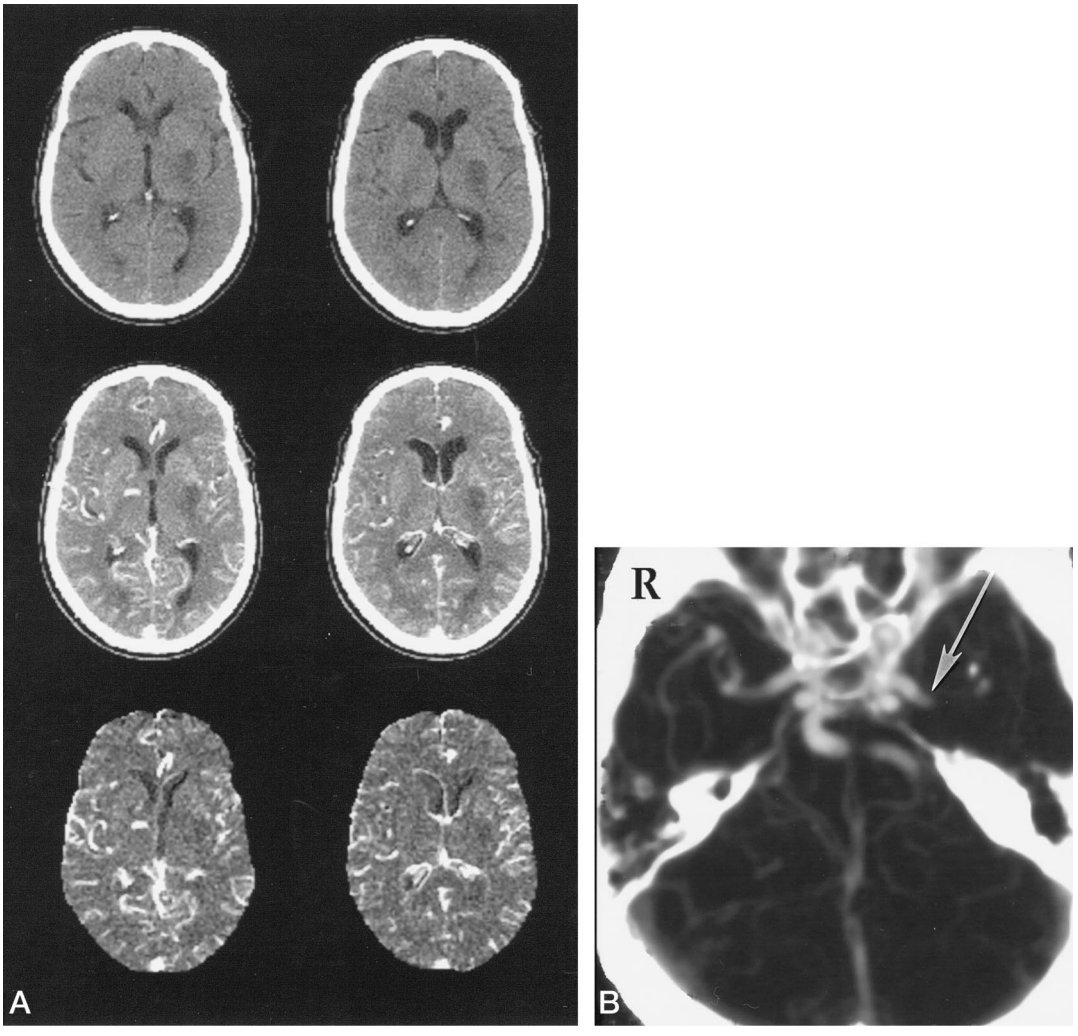

FIG 4. Patient 13.

A, Axial noncontrast (*upper row*) and contrast-enhanced (*middle row*) CT scans, and subtraction PBV maps (*bottom row*). A low-attenuation lesion is seen on the noncontrast CT scans in the left putamen and internal capsule. This lesion is also seen on the contrast-enhanced scans, but is less conspicuous on the subtraction PBV maps.

B, Maximum intensity projection reconstruction from a CT angiogram shows abrupt cutoff of the left MCA (*arrow*).

results in increased capillary recruitment, which in conjunction with dilated arteries gives rise to an increase in the cerebral blood vessel capacity, or cerebral blood volume (CBV), in an area of hypoperfusion. The ability to measure this parameter, however, is determined by the delivery of blood-borne contrast material to these dilated vessels and is largely dependent on CBF. The arrival of contrast agent in a region of normal perfusion is characterized by a proportionality and dependency between CBV and CBF (20). However, in the context of interrupted blood flow, while CBF falls, CBV may increase (20). When CBF falls, contrast delivery is reduced, and thus a decreased contrast density is observed. This observation suggests that we are not measuring the true capacity of the blood vessels (CBV), which one would expect to be maximally dilated, but instead the delivery of contrast material to those vessels that still receive blood, despite ischemia or infarction. For this reason, we refer to *perfused* CBV (PBV) rather than CBV, as we believe it more accurately describes the parameter measured by 3-D functional CT. It should be noted that PBV probably remains proportional to CBF, even in the context of the maximally dilated blood vessels present during ischemia or infarction. In occlusion, with a reduced delivery of blood, both CBF and PBV are low, while vessel capacity (CBV) may be high. This is an example of uncoupling between CBV and CBF (21). It is probable that PBV represents physiologically useful perfusion in the brain, whether measured in well-vascularized or ischemic regions.

When obtaining the data necessary to construct PBV maps, care must be taken to consider the effect of collateral channels on the opacification of different regions of the brain. Proximal occlusion or stenosis may delay the arrival of contrast agent beyond the time of CT acquisition. This may lead to an underestimation of the true PBV and result in an over interpretation of infarction or ischemia. Such a situation could exist where there is carotid occlusion with contralateral carotid blood supply to the ipsilateral hemisphere or in areas of reduced perfusion.

The observation of collateral vessels is possible

Lesional findings in 22 patients studied with three-dimensional functional CT

Case	Noncontrast CT	Contrast-Enhanced CT	CT Angiography	Perfused Cerebral Blood Volume Map
1	Frontal lobe mass	Superior sagittal sinus attenuation	Superior sagittal sinus	Normal
2	Normal	Normal	Normal	Normal
3	SAH	Normal	PICA aneurysm	Normal
4	Cerebellar atrophy	Normal	Normal	Normal
5	Normal	L paraclinoid aneurysm	L paraclinoid aneurysm	Normal
6	L ICA aneurysm	L ICA aneurysm	L ICA aneurysm	Normal
7	Normal	R intracavernous, ICA aneurysm	R intracavernous, ICA aneurysm	Normal
8	Atrophy	Atrophy	Normal	Normal
9	Normal	L ICA aneurysm	L ICA aneurysm	Normal
10*	L corona radiata, thalamus, forceps major, and R motor strip	L corona radiata, thalamus, forceps major, and R motor strip	Normal	L corona radiata, thalamus, forceps major, and R motor strip
11*	Normal	R thalamus	Normal	R thalamus
12*	L cerebellar hemisphere	L cerebellar hemisphere	Normal	L cerebellar hemisphere
13*	L putamen	L putamen	Normal	L putamen
14*	Normal	L basal ganglia		L basal ganglia
15*	R thalamus and posterior parietal lobe	R thalamus and posterior parietal lobe	Normal	R thalamus and posterior parietal lobe
16*	R occipital lobe, thalamus, and posterior limb of internal capsule	R occipital lobe, thalamus, and posterior limb of internal capsule	Irregularity of R P1	R occipital lobe, thalamus, and posterior limb of internal capsule
17*	L internal capsule, basal ganglia, and insular cortex	L internal capsule, basal ganglia, and insular cortex	Cutoff L MCA with collateralization	L internal capsule, basal ganglia, and insular cortex
18†	L cerebellar hemisphere	L cerebellar hemisphere	Basilar artery thrombosis with collateralization	L cerebellar hemisphere
19†	Normal	R cerebral peduncle	Basilar artery thrombosis with collateralization	R cerebral peduncle
20†	Dense R MCA	R ACA and MCA territories	Cutoff R ACA and distal MCA without distal collateralization	R ACA and MCA territories
21†	Bilateral cerebral hemisphere, old; dense R MCA	R corona radiata	Cutoff R MCA with collateralization	R corona radiata
22†	R internal capsule, old	Posterior L temporal lobe	Normal	Posterior L temporal lobe

Note.—SAH indicates subarachnoid hemorrhage; PICA, posterior inferior cerebellar artery; ICA, internal carotid artery; MCA, middle cerebral artery; and ACA, anterior cerebral artery.

* Mature stroke.

† Hyperacute stroke.

with CT angiography because this technique is a snapshot of all vessels simultaneously filled with contrast material. Conventional angiography, on the other hand, shows serial filling of the vessels and does not always identify retrograde filling by collateral flow unless multiple vessels are studied. This situation is exemplified in Figure 1, in which a distal basilar thrombus was seen extending into the left posterior cerebral artery on the CT angiogram but not on the conventional angiogram.

Evaluation of the raw scans, as they appear on the console, may lead to an incomplete understanding of the true state of a patient's cerebral vasculature and parenchymal perfusion. In two of our patients with hyperacute stroke, baseline scans showed a dense middle cerebral artery (MCA), consistent with acute thrombosis. In one case, however, CT angiography revealed a lack of significant collateralization in the right distal MCA territory (Fig 3), while in the other, good collateralization was shown (Fig 2). Furthermore, the PBV maps indicated the effectiveness of this collateralization by demonstrating the extent of residual, adequately perfused brain in the territory of the proximally occluded vessel. The first case shows an extensive perfusion deficit (Fig 3), while the other shows a much smaller perfusion deficit, despite similar occlusion of the involved MCA (Fig 2). These data suggest that the combination of CT angiography and PBV available with 3-D functional CT can provide a powerful means of quantifying the true volume of brain at risk from hypoperfusion. In case 22 (Fig 5), evaluation of the noncontrast and contrast images prospectively, together with the CT angiographic findings, revealed that this patient did not need to proceed to thrombolytic therapy. This assessment took less than 20 minutes and was performed by the neuroradiology, neurology, and neurointerventional radiology teams in the emergency department while the patient was still in the CT scanner. As there was no indication for thrombolysis, triage was to MR imaging and conventional medical therapy. The MR study was performed within 4 hours and confirmed

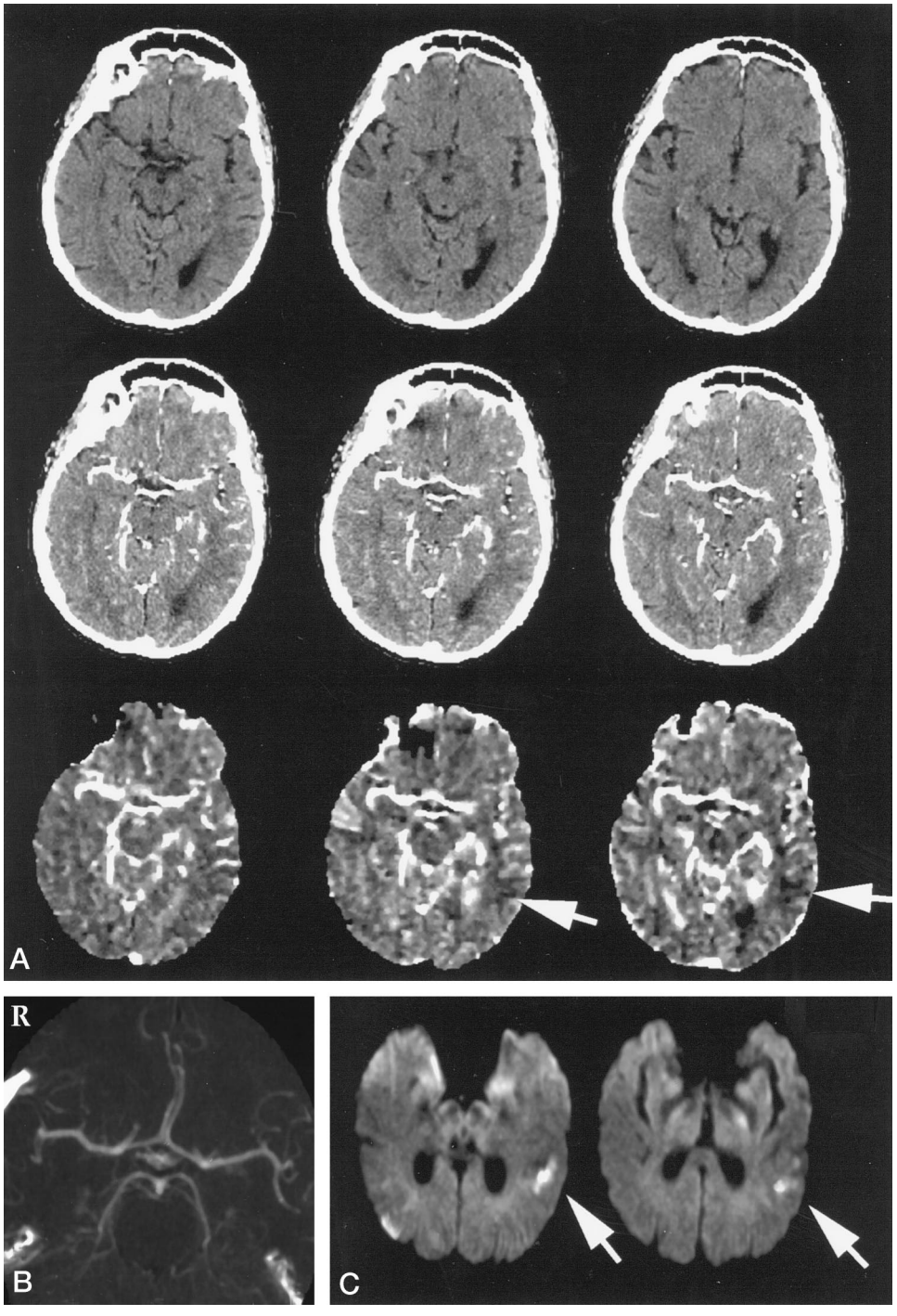

FIG 5. Patient 22.

A, Axial noncontrast (*upper row*) and contrast-enhanced (*middle row*) CT scans, and subtraction PBV maps (*bottom row*). Abnormal low attenuation is seen in the left posterior temporal region on the contrast-enhanced scans and the PBV maps (*arrows*). PBV was 0.55 ± 0.07%. This finding is compatible with a watershed infarction.

B, Collapsed multiprojection volume reconstruction shows the absence of major-vessel occlusion.

C, Diffusion-weighted axial MR images obtained 4 hours later confirmed the location of the acute infarction. *Arrows* correspond to those on the PBV maps in *A*.

the CT findings. MR imaging was not performed before CT simply because this would have introduced an unacceptable delay in triage of this patient.

Conclusions

We have implemented a straightforward and cost-effective method of evaluating quantitative regional perfusion in the whole brain by using a CT angiography protocol with tailored software analysis to produce maps of PBV and major-vessel CT angiograms. As most stroke patients currently undergo CT to exclude hemorrhage, the addition of a helical scan during contrast infusion introduces a delay of only a few minutes and provides PBV and CT angiographic data. The combination of CT angiography and PBV permits simultaneous assessment of collateralization and the actual volume of brain parenchyma that remains at risk from an ischemic event.

Acknowledgments

We express our appreciation to JoAnne Fordham for her invaluable assistance in preparing the manuscript. Grateful thanks is also extended to the Neuroradiology Fellows and

Neurology Residents, without whom this study would not have been possible.

References

1. The National Institute for Neurological Disorders and Stroke, rt-PA Stroke Study Group. **Tissue plasminogen activator for acute ischemic stroke.** *N Engl J Med* 1995;333:1581–1587
2. Adams HP, Brott TG, Furlan AJ, et al. **Guidelines for thrombolytic therapy for acute stroke: a supplement to the guidelines for the management of patients with acute ischemic stroke.** *Stroke* 1996; 27:1711–1718
3. The Multicenter Acute Stroke Trial-European Study Group. **Thrombolytic therapy with streptokinase in acute ischemic stroke.** *N Engl J Med* 1996;335:145–150
4. Hacke W, Kaste M, Fieschi C, et al. **Intravenous thrombolysis with recombinant tissue plasminogen activator for acute hemispheric stroke: the European Cooperative Acute Stroke Study (ECASS).** *JAMA* 1995;274:1017–1025
5. Hamberg LM, Hunter GJ, Halpern EF, Hoop B, Gazelle GS, Wolf GL. **Quantitative, high resolution measurement of cerebral vascular physiology with slip-ring CT.** *AJNR Am J Neuroradiol* 1996;17: 639–650
6. Hamberg LM, Hunter GJ, Kierstead D, Lo EH, Gonzalez RG, Wolf GL. **Measurement of quantitative CBV with subtraction three-dimensional functional CT.** *AJNR Am J Neuroradiol* 1996;17: 1861–1869
7. Hunter GJ, Hamberg LM, Morris PP, et al. **Demonstration of the cerebrovascular physiology of acute stroke using high resolution first pass slip-ring CT. In:** *Proceedings of the Annual Meeting of the American Society of Neuroradiology.* Oak Brook, Ill: American Society of Neuroradiology; 1995:38
8. Sakai F, Nakazawa K, Tazaki Y, et al. **Regional cerebral blood volume and hematocrit measured in normal human volunteers by single-photon emission computed tomography.** *J Cereb Blood Flow Metab* 1985;5:207–213
9. Gado MH, Phelps ME, Coleman RE. **An extravascular component of contrast enhancement in cranial computed tomography.** *Radiology* 1975;117:589–593
10. Penn RD, Walser R, Ackerman L. **Cerebral blood volume in man: computer analysis of a computerized brain scan.** *JAMA* 1975;234: 1154–1155
11. Sabatini U, Celsis P, Viallard G, Rascol A, Marc-Vergens J-P. **Quantitative assessment of cerebral blood volume by single-photon emission computed tomography.** *Stroke* 1991;22:324–330
12. Hunter GJ, Hamberg LM, Wolf GL, Gonzalez RG. **Measurement of blood volume and blood flow in the entorhinal cortex using slip-ring computed tomography.** In: *Proceedings of the Annual Meeting of the American Society of Neuroradiology.* Oak Brook, Ill: American Society of Neuroradiology; 1995:169
13. Camarata PJ, Heros PC, Latchaw RE. **Brain attack: the rationale for treating stroke as a medical emergency.** *Neurosurgery* 1994; 34(Suppl 1):144–158
14. Heiss WD, Rosner G. **Functional recovery of cortical neurones as related to degree and duration of ischemia.** *Ann Neurol* 1983;14: 294–301
15. Heiss WD. **Experimental evidence of ischemic thresholds and functional recovery.** *Stroke* 1992;23:1668–1672
16. Rosovsky MA, Rusinek H, Berenstein A, Basak S, Setton A, Nelson PM. **High-dose administration of nonionic contrast media: a retrospective review.** *Radiology* 1996;200:119–122
17. Hunter JV, Kind PR. **Nonionic iodinated contrast media: potential renal damage assessed with enzymuria.** *Radiology* 1992;183:101–104
18. Symon L, Ganz JC, Dorsch NWC. **Experimental studies of hyperaemic phenomena in the cerebral circulation of primates.** *Brain* 1972;95:265–278
19. Gourley JK, Heistad DD. **Characteristics of reactive hyperemia in the cerebral circulation.** *Am J Physiol* 1984;246(*Heart Circ Physiol* 15):H52–H58
20. Todd NV, Picozzi P, Crockard HA. **Quantitative measurement of cerebral blood flow and cerebral blood volume after cerebral ischemia.** *J Cereb Blood Flow Metab* 1986;6:338–341
21. Tasdemiroglu E, Macfarlane R, Wei EP, Kontos HA, Moskowitz MA. **Pial vessel caliber and cerebral blood flow become dissociated during ischemia/reperfusion in cats.** *Am J Physiol* 1992;263:H533–H536

Please see the Editorial on page 191 in this issue.